Homotopic Approach for the Simulation of DC-DC Power Electronic Converters

Guillermo Gallo[1] Hector Vazquez-Leal[2]
Victor M. Jimenez-Fernandez[3] Gustavo Osorio[4]
Fabiola Angulo[5] Jose A. Martinez-Melchor[6]

(Received 31 May 2018; revised 8 December 2018)

Abstract

This paper presents three homotopic methods to determine the suitable topology to be simulated in DC–DC power electronic converters. One of the proposed methods is based on Newton and hyperspheres tracking, by using the canonical piecewise-linear model of Chua–Kang to represent the characteristic curve of the diodes. The other two homotopic methods are based on fixed point and Newton with uniform variation of the homotopic parameter, by using hybrid diode models. Numerical simulations via MATLAB were compared with the results obtained from PLECS, and a good agreement was found between both simulation alternatives.

DOI:10.21914/anziamj.v60i0.13250, Published 2018-12-18. ISSN 1445-8810. (Print two pages per sheet of paper.)

*The corresponding author is Victor M. Jimenez-Fernandez.

Subject class: 65H20

Keywords: homotopy; power converter; event-driven simulation; hybrid system

Contents

1 Introduction

Electronic power converters are devices that continuously switch between different circuit topologies [26, 11, 13]. In general, 2^n topologies can be

Figure 1: (a), Buck converter schematic; (b)–(d), physically possible topologies

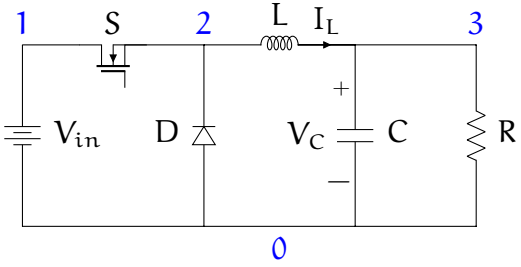

(a) Buck converter

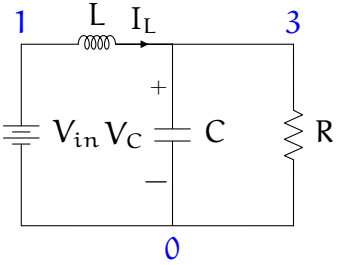

(b) S = ON, D = OFF

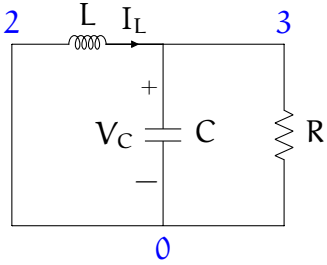

(c) S = OFF, D = ON

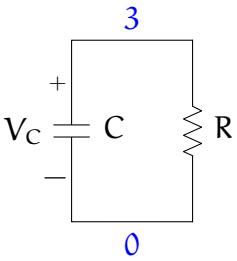

(d) S = OFF, D = OFF

presented in a converter, where n is the number of semiconductors (switching diodes and transistors), each topology is determined by the states OFF and ON of the switches [26, 25, 5, 8]. For example, the Buck converter depicted in Figure 1 presents four topologies depending on the state of the transistor S and the diode D. However, only three topologies are physically possible [10].

From the context of the simulation, it is important to determine adequately in which topology the converter is operating for certain initial conditions [5, 8]. The determination of the appropriate topology must be made before starting the simulation and each time a switch is detected, as a switch can trigger the occurrence of others [11, 13, 12]. Most of the technical literature in power electronics simulation lacks theoretical and analytical approaches to

predict the state of the semiconductors after switching [26, 11, 13]. There are heuristic methodologies that basically test which is the most consistent topology of the 2^n possible [26]. Alternatively, there are some analytical approaches that work but they are not used because they are less efficient; for instance, the extra element theorem [22]. Another analytical approach is the compensation theorem [12], which requires tools of symbolic analysis. We propose the use of homotopic continuation methods to predict the state of the semiconductors after switching. The homotopy has never been used for this purpose.

In accordance with Collins [9]: two mathematical objects are said to be homotopic if one of them is capable of continuously deforming to the other one [4, 17, 19]. Our proposal consists of considering a power electronic converter as a finite set of continuous subsystems or circuit topologies where each topology is regarded as a continuous deformation of any other topology. Understanding each semiconductor of a converter as a variable resistor that could take a value that tends to zero or infinity according to its state of conduction (ON, OFF), it might be thought that the transitions between the different circuit topologies are the result of a homotopic process in which the resistors associated with the semiconductors are deformed from 0 to ∞ or vice versa. For example, the Buck converter is modelled as a homotopic system as shown in Figure 2. The transitions in Figure 2 are determined by the deformations of the transistor resistance (R_S) and the resistance of the diode (R_D).

The homotopy has already been used for other applications such as solving nonlinear partial differential equations and free boundary problems [31], solving systems of nonlinear algebraic equations [18, 20] and DC analysis of electrical circuits [20, 21, 24, 27, 28, 29]. However, the homotopic continuation problems have never been used to solve the problem of detecting the proper topology in an electronic converter after switching. Three homotopic methods are proposed. The first one uses the canonical representation of Chua–Kang for diode description, which is a piecewise smooth linear model (Section 3). The remaining two homotopic methods use a hybrid diode model, which gen-

Figure 2: Buck converter as homotopic system.

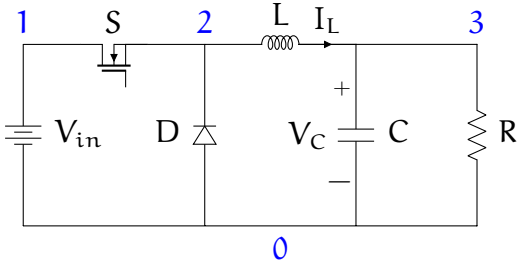

(a) Buck converter.

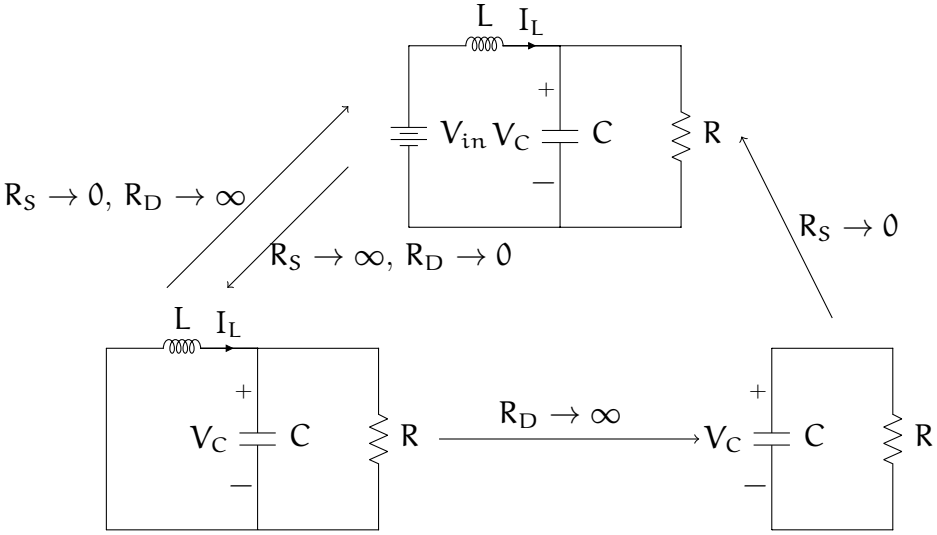

(b) Homotopic system.

erates a set of linear circuit topologies (Section 4). Unlike traditional heuristic methods that use a trial and error strategy, the proposed homotopic methods describe an intuitive explanation of how a converter transits through different topologies. Thus, the main advantage offered by homotopic continuation methods is that they trace a clear and deterministic path for the handling of semiconductor switching; this feature facilitates the elaboration of the algorithms. The purpose of this article is not to compare homotopic continuation techniques with those that currently exist in terms of computational speed. The purpose is to validate the hypothesis of how a converter is understood as a homotopic system, and in this way to offer an alternative technique for handling commutations, which could be optimised in the future.

Figure 3 depicts the proposed simulation scheme. The first step is to read the parameters and the description of the circuit through a schematic diagram or a NETLIST. Then the equations of the system are generated by modified nodal analysis [25]. Subsequently, the most suitable circuit topology is calculated by means of a homotopic continuation technique. Finally, the system of equations is integrated until some commutation occurs [12, 11]. After the detection of the switching, the cycle must be repeated; first calculating a new topology and then integrating it until the integration time ends. This article focuses on the task of finding the appropriate topology to simulate an electronic converter; given some initial conditions (dashed block, Figure 3). The tasks of generating the equations of the system and integrating them numerically have been studied extensively [25, 26, 16].

To validate the proposed homotopic methods, some simulations of three converters have been replicated: Boost [2], Boost–Flyback [14] and a Boost of high gain [30]. We performed MATLAB-based simulations using the three proposed homotopic algorithms for handling commutations. We also implemented in MATLAB the trial and error algorithm proposed by Gallo [15]. Finally, the converters were implemented in the commercial PLECS software, which is a simulator of electrical circuits specialised in power electronics [26]. PLECS is a hybrid simulator that generates each circuit topology as switching is detected by means of a *switch manager*. For a better understanding of

Figure 3: Simulation scheme.

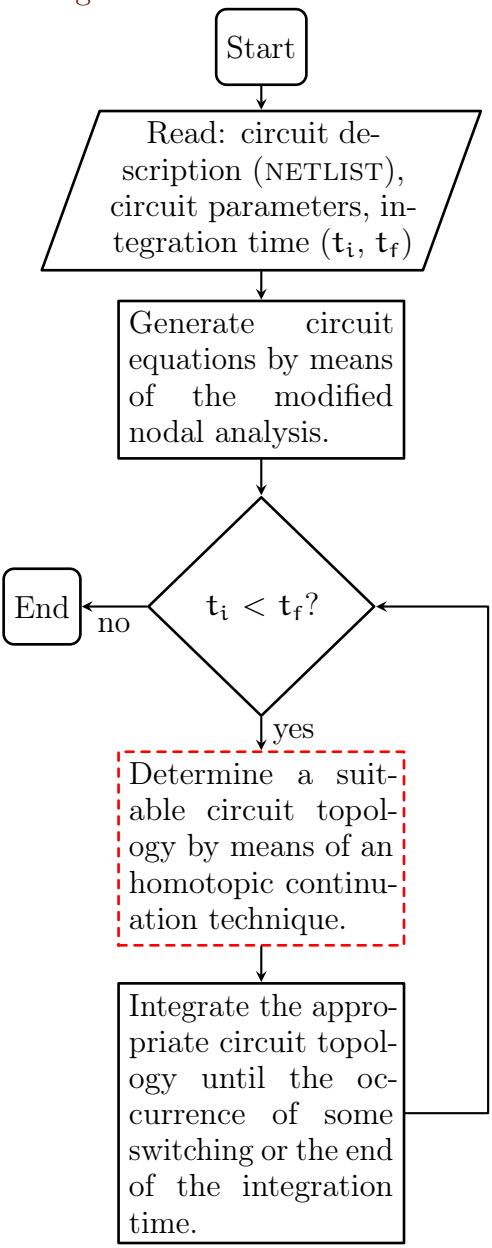

PLECS see Alimeling [1]. Section 5 presents a time simulation comparison.

2 Continuation methods and homotopic path tracking

This section provides a brief description of Newton and fixed point homotopies as well as explaining the technique of hyperspheres path tracking.

In general terms, homotopy is used to solve systems of nonlinear algebraic equations of the form

$$f(x) = 0, \quad f \in \mathbb{R}^n \to \mathbb{R}^n. \tag{1}$$

The homotopic continuation methods perturb the system $f(x)$ by adding a homotopic parameter λ and a function $G(x)$ whose solution is known or easily calculable. In this way, a continuation problem is expressed as

$$H(f(x), \lambda) = \lambda f(x) + (1 - \lambda) G(x) = 0, \quad H \in \mathbb{R}^n \times \mathbb{R} \to \mathbb{R}^n. \tag{2}$$

By solving (2), a set of solutions that describe the homotopic curve is obtained. Figure 4 illustrates these solutions.

If $\lambda = 0$, then $H(f(x), 0) = G(x)$; which means that the solution of the system is trivial or easy to calculate. In contrast, if $\lambda = 1$, then $H(f(x), 1) = f(x)$; which represents the left-hand side of the original system. This means that the solutions of the original system coincide with the intersection of the homotopic curve when $\lambda = 1$.

There are different ways to obtain a function $G(x)$ that has a trivial solution. For example, if $g(x) = x - x_i$, then a **fixed point homotopy** is obtained:

$$H(f(x), \lambda) = \lambda f(x) + (1 - \lambda)(x - x_i) = 0, \tag{3}$$

Figure 4: Homotopic curve: x_1^* and x_2^* are the solutions of the system.

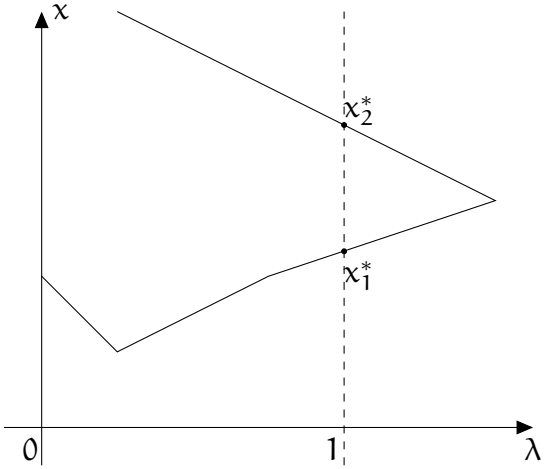

where x_i is any initial condition where the homotopic curve begins. Another alternative for is $G(x) = f(x) - f(x_i)$; generating the **Newton homotopy**,

$$H(f(x), \lambda) = f(x) + (\lambda - 1) f(x_i) = 0. \tag{4}$$

In both, the fixed-point and Newton homotopy, the resulting system has n equations and $n + 1$ variables. An alternative to solve the problem of continuation is to gradually vary the parameter λ from 0 to 1 in order to find the solution of the system. Another alternative used in DC circuit analysis is to propose a last equation that corresponds to a hypersphere [27, 24, 28],

$$\begin{aligned} S(x_1, x_2, \cdots, x_{n+1}) = (x_1 - c_1)^2 + (x_2 - c_2)^2 + \cdots \\ + (x_{n+1} - c_{n+1})^2 - r^2 = 0. \end{aligned} \tag{5}$$

where $x_{n+1} = \lambda$, r and c are the radius and centre of the hypersphere. Adding (5) to the continuation problem $H(f(x), \lambda) = 0$, an increased system of algebraic equations is obtained:

$$H(f(x), \lambda) = 0, \quad \text{and } S_k(x, \lambda) = 0. \tag{6}$$

Figure 5: Hyperspheres homotopic path tracking.

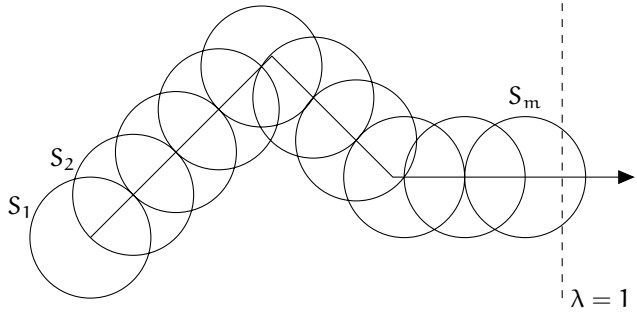

(a) Homotopic curve.

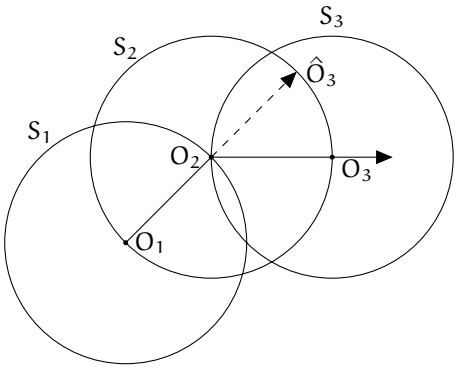

(b) Predictive scheme.

A homotopic curve is traced by solving (6) as shown graphically in Figure 5. In accordance with this solution strategy, each hypersphere must be individually solved and the obtained data must be used as the centre of the next hypersphere. The subscript k refers to kth hypersphere. The path tracking procedure consists of two steps: a predictive and a corrective. Figure 5(b) describes the predictive procedure [27] whose basic idea is explained as follows: with the centres of two previous hyperspheres (O_1 and O_2), a vector that estimates the centre of the next hypersphere ($\hat{O}_3$) is calculated. Then, a

corrective procedure, which consists of solving the system (6) is applied. It is possible that when the homotopic curve crosses $\lambda = 1$ the centre of the hypersphere does not exactly coincide with that point. In this case, system (1) must be solved to accurately determine the root of the original system; another alternative is to use any interpolation algorithm.

3 Hyperspheres homotopic path tracking algorithm for piecewise linear circuits simulations

In this section the problem of hyperspheres homotopic path tracking is applied to the prediction of the state of the switches (transistors and diodes) in power electronic converters whose diodes are modelled as piecewise linear resistors [7]. Section 3.1 explains briefly the diode model wich is based on the canonical piecewise representation of Chua–Kang. Section 3.2 presents the proposed homotopic method. Some illustrative examples are given in Section 3.3.

3.1 Piecewise linear model of Chua–Kang

This homotopic technique uses the canonical piecewise linear model of Chua–Kang to describe the characteristic V-I curve of the diode [6]. Figure 6 depicts a piecewise linear curve composed by two straight lines and a break point at the origin. This curve represents a two-line segment approximation of a diode. The first straight line is defined in the interval $(-\infty, 0]$ with a slope $1/R_B$, where R_B is a very large resistance related with the blocking state of the diode. The second straight line is defined in the interval $[0, \infty)$ with a slope $1/R_C$, where R_C is a very small resistance associated with the conducting state of the

Figure 6: Diode characteristic curve.

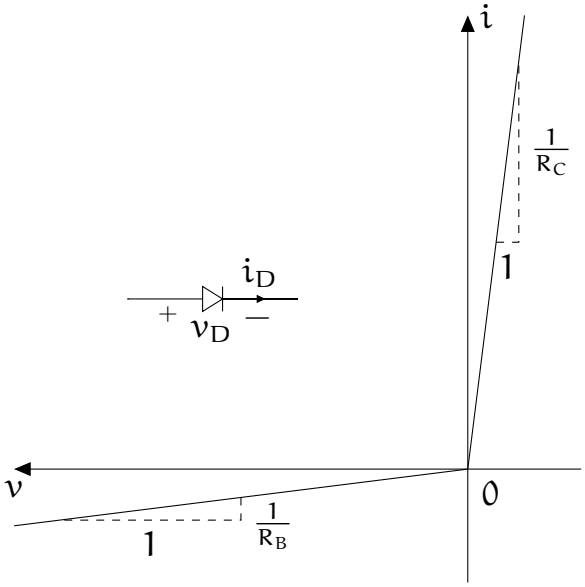

diode. After using the canonical model of Chua–Kang the function $f_D(v_D)$ is

$$i_D = f_D(v_D) = \frac{1}{2}\frac{R_B + R_C}{R_B R_C} v_D + \frac{1}{2}\frac{R_B - R_C}{R_B R_C} |v_D| . \tag{7}$$

3.2 Newton homotopy with hyperspheres path tracking

Here, a homotopic technique is proposed in order to detect the state of the semiconductors after switching. Given a commutation in a converter, it is possible to determine the state of the semiconductors by solving the following homotopic continuation problem:

$$H(x, \lambda) = f_C(x) + (\lambda - 1) f_C(x_i) = 0 ,$$

$$S_k(x,\lambda) = (x_1 - c_{k_1})^2 + (x_2 - c_{k_2})^2 + \cdots + (x_n - c_{k_n})^2 + (\lambda - c_{k_{n+1}})^2 - r^2 = 0\,, \tag{8}$$

where f_C is the system of algebraic equations that models the converter; $k \in \{1, 2, \ldots, m\}$; m is the number of hyperspheres; c_k is the centre of the kth hypersphere; r is the radius of the hyperspheres; x_i is the initial condition of the homotopic continuation problem; this value is selected according to the criteria established by Ramirez-Pinero [24]. The basic idea of this technique is to select initial voltages and currents that are equal or superior to the maximum sources of voltage and current presented in the circuit. For example, in a step-up converter all initial voltages must be equal or greater than the output voltage.

3.3 Cases of study

In order to test the proposed homotopic tracking technique, two cases of study are presented: the Boost and Boost–Flyback converters. In these circuits, only the nodal voltages are of interest since basically these determine the commutations of diodes. For both circuits, we set the resistance of conduction and blocking of the diodes to $R_C = 1\,\mu\Omega$ and $R_B = 1\,M\Omega$.

3.3.1 Boost converter

Boost converter is capable of raising voltage levels [2, 3]. Figure 7 shows the schematic diagram of the Boost converter. The control law that determines the switching of the transistor and parameters were taken from El Aroudi [2]. The control law is

$$U = \begin{cases} 1 & \text{if } V_C \geqslant V_S\,, \\ 0 & \text{if } V_C < V_S\,, \end{cases}$$

Figure 7: Boost converter.

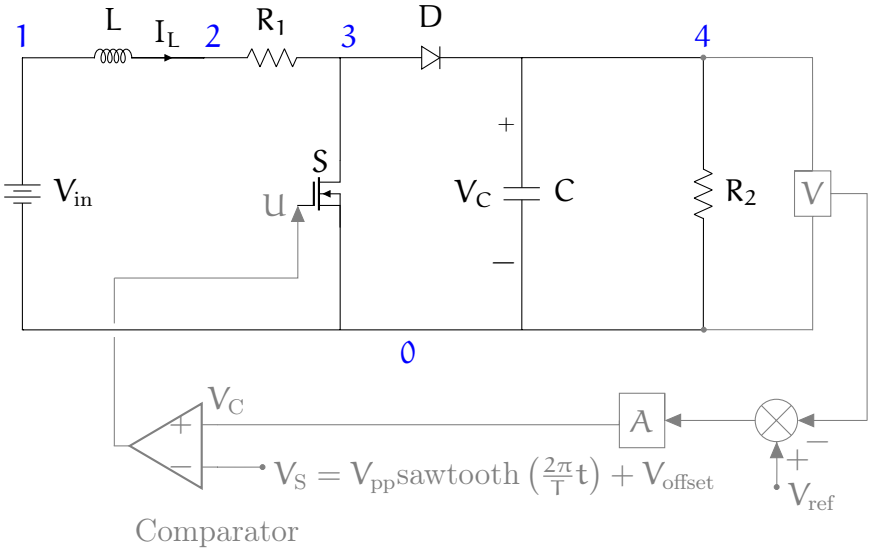

where

$$V_C = A\,(V_{ref} - V_4)\,; \quad V_S = V_{pp}\text{sawtooth}\left(\frac{2\pi}{T}t\right) + V_{offset};$$
$$V_{pp} = \frac{V_u - V_l}{2}; \quad V_{offset} = \frac{V_u + V_l}{2}.$$

Here, A is a voltage gain, and V_l and V_u are respectively the minimum and maximum voltage that a control signal can take. The sawtooth signal behaves as shown in Figure 8 and is

$$y = \text{sawtooth}\left(2\pi\frac{t}{T}\right). \tag{9}$$

The sawtooth signal has a periodic behaviour similar to a sine or cosine signal. Furthermore, this function is defined in the same way as it operates in MATLAB. The parameters of the circuit are $V_{in} = 30\,V$, $R = 22\,\Omega$, $L = 20\,mH$,

Figure 8: Sawtooth signal.

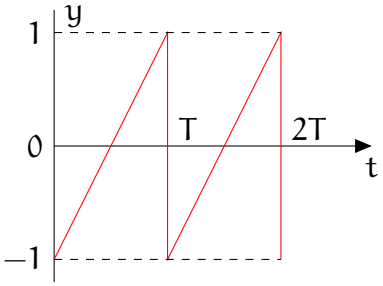

$C = 47\,\mu F$, $T = 400\,\mu s$, $V_l = 3.8\,V$, $V_u = 8.2\,V$, and $A = 8.4$. It is important to try to make the radius of the hyperspheres as large as possible to accelerate the simulations, we found that with $r = 0.3$ stable simulations were obtained. Three cycles of $T = 0.4\,ms$ were simulated with the following initial conditions: $V_{C_0} = 8.12\,V$, $I_{L_0} = 0.04\,A$. These initial conditions are contained in a quasi-periodic orbit [2]. Figure 9(a)(c)(e)(g) illustrate simulations over time; the red marks denote the points at which the switching of some semiconductor occurs. There were altogether six commutations, for each of them the homotopic continuation problem was solved to find the next circuit topology. However, only the results of the homotopic continuation are illustrated for one of the six commutations. The black circumference encloses the commutation occurred in $0.8\,ms$, for this instant of time the homotopic procedure has been illustrated to find the next state of the semiconductors, Figure 9(b)(d)(f)(h). The initial conditions of the homotopic problem should be set equal to or greater than the values of the voltage and current sources, as established by Ramirez–Pinero [24]. All voltages of the homotopic problem start at the output voltage and, by means of the homotopic continuation technique, they converge to their final value in $\lambda = 1$; these final values correspond to those observed in the temporal simulations and determine the state of the semiconductors. For example, for voltage V_3 Figure 9(e)(f) shows that just before a commutation, in $t = 0.8^-\,ms$, the voltage was around $7\,V$. At the end of the homotopic process, in $\lambda = 1$, the voltage reaches its final

Figure 9: Time simulation of the Boost converter: (a)(c)(e)(g), red circles, switching points; (b)(d)(f)(h), homotopic continuation for detect next circuit topology in $t = 0.8$ ms.

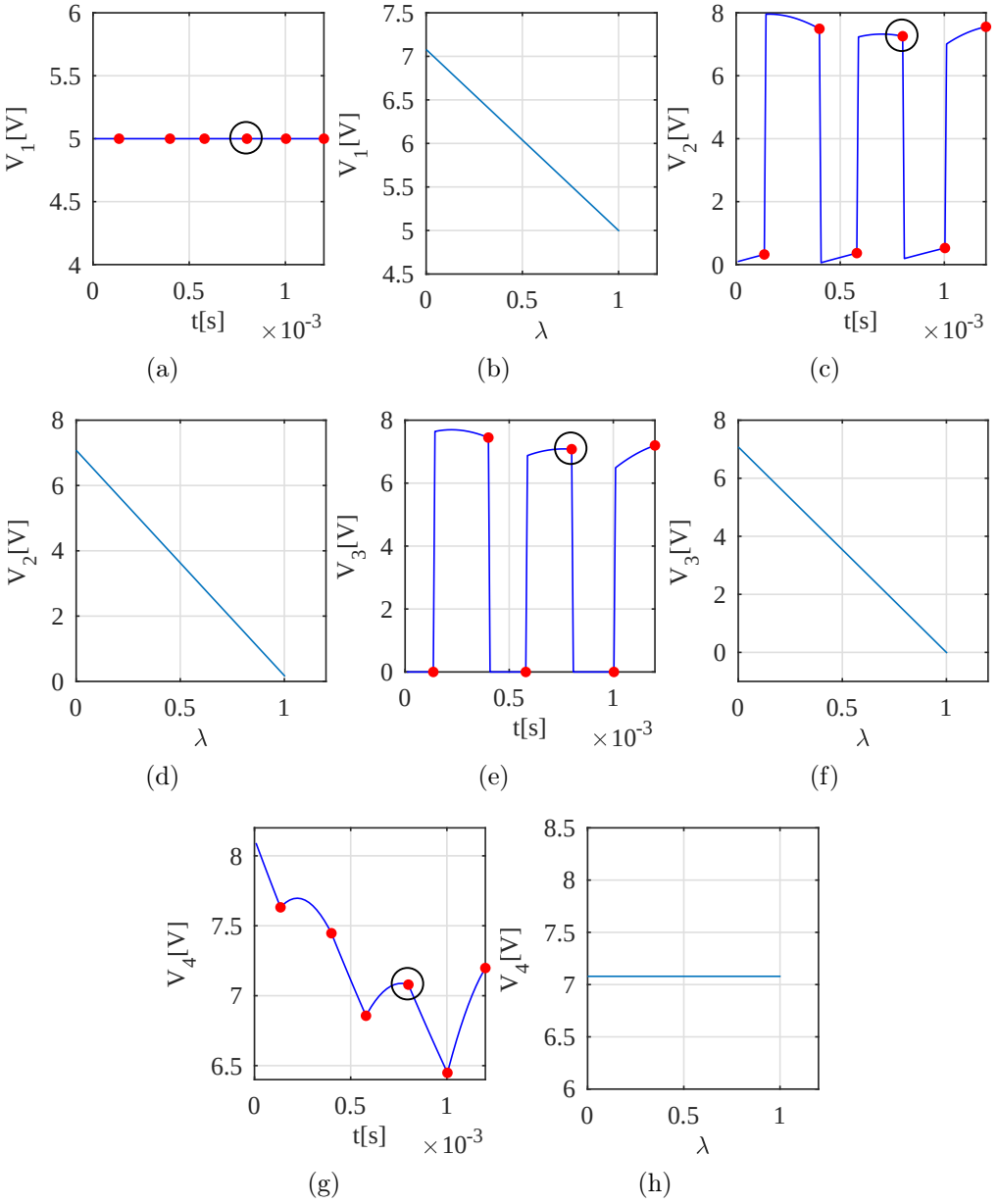

Table 1: Table of time transitions of the Boost converter.

		Next Topology	
Time [ms]	Switching element	D	S
0.1353	S	1	0
0.4000	S	0	1
0.5796	S	1	0
0.8000	S	0	1
1.0000	S	1	0

value of $V_3\,(t = 0.8^+\,\text{ms}) = 0\,\text{V}$. Table 1 describes chronologically the devices that switched and the topologies to which it was transited by means of the homotopic procedure. All simulations were also performed in PLECS obtaining closely similar results.

3.3.2 Boost–Flyback converter

Boost–Flyback converter is capable of raising voltages with good efficiency (about 90%) [14, 23]. Figure 10 shows the schematic of the Boost–Flyback converter. In this example, the circuit parameters were taken from Florez [14]. The converter was simulated in open loop at a 50% duty cycle. The parameters of the circuit are $V_{in} = 5\,\text{V}$, $R = \begin{bmatrix}1.27\,\Omega & 2.7\,\Omega & 100\,\Omega\end{bmatrix}$, $L = \begin{bmatrix}183\,\mu\text{H} & 724\,\mu\text{H}\end{bmatrix}$, magnetic coupling constant $k = 0.996$, $T = 200\,\mu\text{s}$, $C = \begin{bmatrix}220\,\mu\text{F} & 220\,\mu\text{F}\end{bmatrix}$. A radius $r = 0.1$ was used for the homotopic tracing routines. A single cycle of $T = 200\,\mu\text{s}$ was simulated with the following initial conditions: $V_{C_0} = \begin{bmatrix}8.38\,\text{V} & 6.62\,\text{V}\end{bmatrix}$, $I_{L_0} = \begin{bmatrix}0\,\text{A} & 0\,\text{A}\end{bmatrix}$.

Time simulations are shown in Figure 11(a)(c)(e)(g)(i) and Figure 12(b)(d). Some switch marks (red dots) overlap, this is because the occurrence of some events could be very close in time (Table 2). The black circumference encloses the commutation occurred in 0.1 ms; for that instant the homotopic continuation routines have been illustrated to detect the next topology, Figure 11(b)(d)(f)(h) and Figure 12(a)(c)(e). As in the previous case study (Sec-

Figure 10: Boost–Flyback converter.

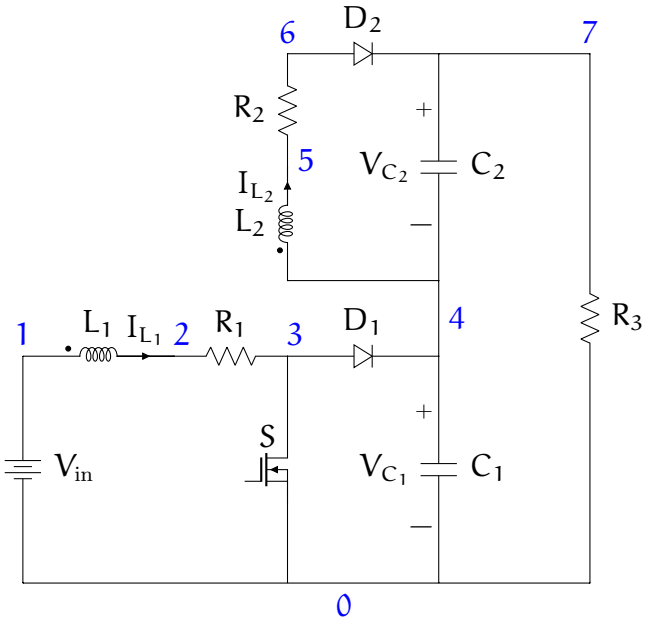

tion 3.3.1), all the voltages start at the output voltage and by means of the homotopy converge to their final value in $\lambda = 1$; these final values correspond to those observed in the time simulations and determine the state of the semiconductors. Table 2 describes chronologically the devices that switched and the topologies to which it was transited. Similarly, as in the previous example, all simulations were contrasted with PLECS obtaining practically the same results.

Figure 11: (a)(c)(e)(g)(i), time simulation of the Boost–Flyback converter where red circlesare switching points; (b)(d)(f)(h), homotopic continuation for detect next circuit topology in $t = 0.8$ ms.

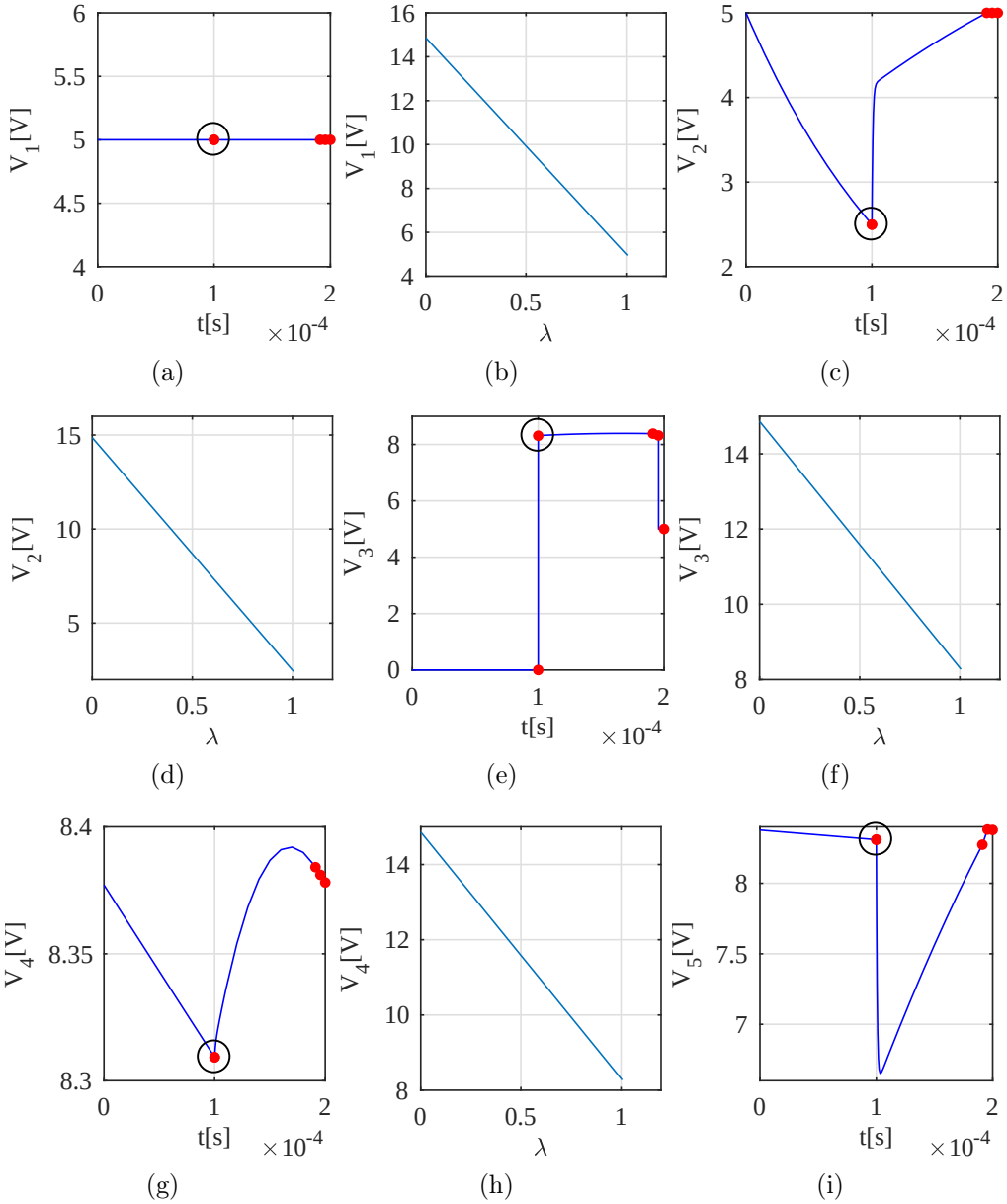

Figure 12: (b)(d), time simulation of the Boost–Flyback converter where r circles are switching points. (a)(c)(e), homotopic continuation for detect next circuit topology in $t = 0.8\,\text{ms}$.

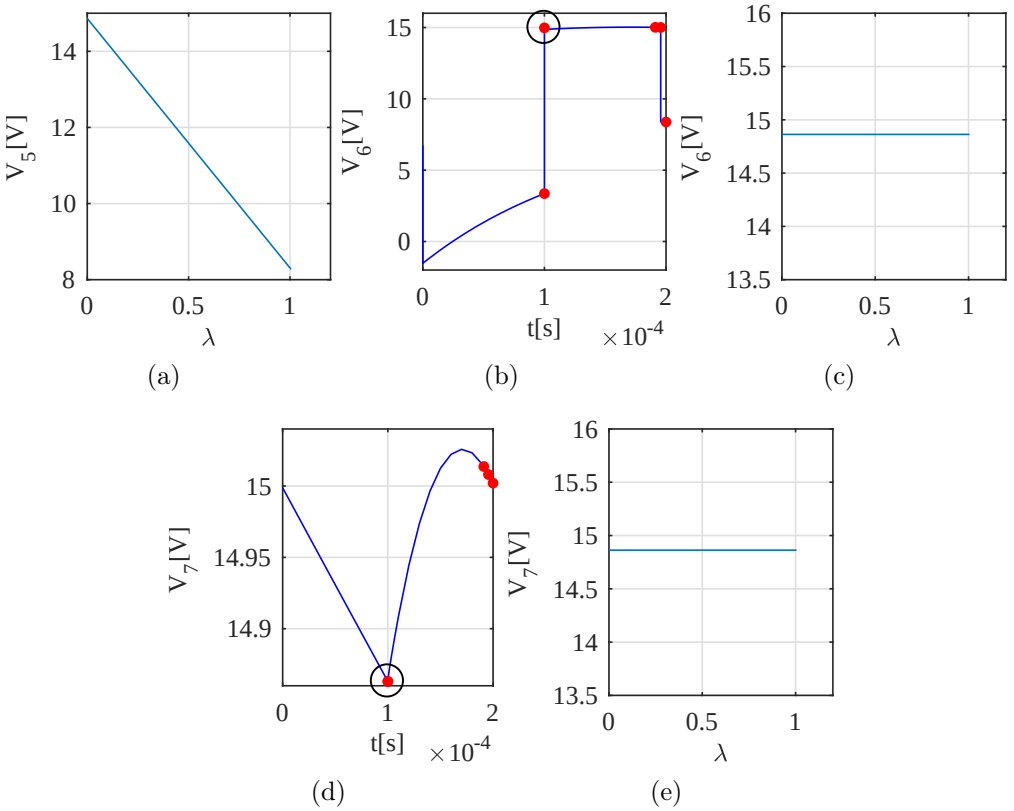

Table 2: Table of time transitions of the Boost–Flyback converter.

		Next Topology		
Time[ms]	Switching element	D_2	D_1	S
0.0999	S	0	1	0
0.1000	D_2	1	1	0
0.1912	D_1	1	0	0
0.1955	D_2	0	0	0

4 Hybrid homotopy

In this section two homotopic continuation techniques are proposed for electronic converters whose diodes are modelled using hybrid systems; this implies the occurrence of 2^n circuit topologies, where n is the number of semiconductors.

4.1 Newton and fixed point homotopy with tracking by uniform variation of parameter

Two homotopic continuation methodologies are presented to detect the proper topology of a converter after some switching has occurred. Both methodologies require the prior knowledge of the device that has been switched. Commutations are of two types: increasing and decreasing. Increasing commutations occur when the device was in the conducting state and switch to the blocking state, assuming an increase of the resistance associated with the semiconductor device. An inverse reasoning is done to determine the decreasing commutations. Given that R_I is the resistance of the switching device ($R_I \in \{R_T, R_{D_1}, R_{D_2}, \ldots, R_{D_{ND}}\}$), where ND is the number of diodes in the circuit, the law that determines the value of this resistance with respect to homotopic parameter λ is defined as

$$R_I = \lambda R_f + (1-\lambda)\, R_i\,. \tag{10}$$

Here, R_i and R_f are respectively the initial and final resistances that the semiconductor takes. If the switching is increasing, then $R_i = R_C$ and $R_f = R_B$, otherwise $R_i = R_B$ and $R_f = R_C$. R_B and R_C are respectively a very large and a very small resistance associated with the conducting and blocking states of the semiconductor device that switches. The methodology for the hybrid simulation is that by Gallo [15]. The system of algebraic equations that model the converter is

$$f_{Hyb}(x) = J_k x + U = 0, \tag{11}$$

where $x = \begin{bmatrix} V & I_V & I_C \end{bmatrix}$, V is a vector of nodal voltages, I_V is a vector of the currents of the voltage sources, and I_C is the vector of the currents of the capacitors. J_k and U are matrices obtained by modified nodal analysis of the circuit in the kth circuit topology [15]. k is the circuit topology in which the converter is operating. Each topology is linear; however, since the system is made up of several topologies that switch between them, the nature of the global system is nonlinear due to the commutations. In this way a fixed-point homotopy is proposed as

$$H(x, \lambda) = \lambda f_{Hyb}(x) + (1 - \lambda)(x - x_i). \tag{12}$$

A **Newton homotopy** is also proposed as

$$H(x, \lambda) = f_{Hyb}(x) + (\lambda - 1) f_{Hyb}(x_i). \tag{13}$$

where x_i is the initial condition just before of switching. Parameter λ increases from $\lambda = 0$ to $\lambda = 1$ with steps of $\Delta\lambda$, $\lambda \in \begin{bmatrix} 0 & \Delta\lambda & 2\Delta\lambda & \cdots & 1 \end{bmatrix}$. For each λ increment the resistance of the switching device (R_I) varies according to (10), deforming a little bit the system (11) and the continuation problem that is being solved: fixed point (12) or Newton (13). Once the continuation problem is solved for a value of λ determined, it should be assessed if one or more of the semiconductors have switched. If there is any switching, then a new topology k has been found. The initial conditions x_i must also be recalculated and restarted the continuation problem from $\lambda = 0$ and with R_i started at the last value that took R_I.

Figure 13: boost converter of high gain of voltage level.

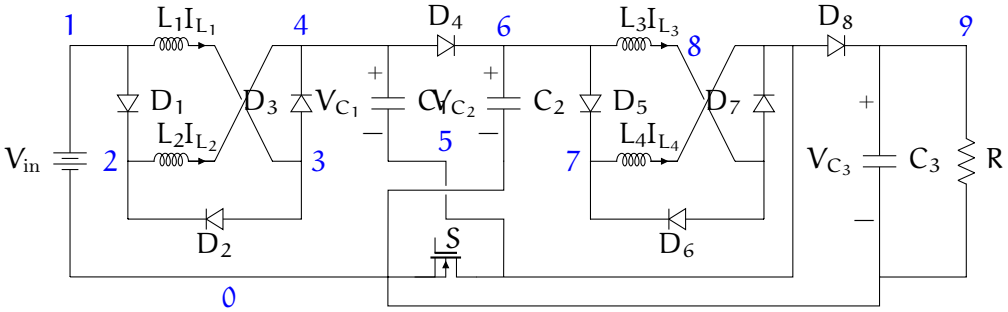

4.2 Case of study: boost converter of high gain of voltage level

This converter is capable of raising voltages at higher levels than a conventional boost converter and using low duty cycles (about 30%) [30]. Figure 13 depicts the schematic diagram of this converter. The parameters were taken from Zhang [30], considering a duty cycle of 30% in simulations. The parameter values are $V_{in} = 20\,V$, $R = 200\,\Omega$, $L = \begin{bmatrix} 330\,\mu H & 330\,\mu H & 330\,\mu H & 330\,\mu H \end{bmatrix}$, $C = \begin{bmatrix} 470\,\mu F & 470\,\mu F & 470\,\mu F \end{bmatrix}$, $T = 20\,\mu s$. For the homotopic routines a step size of $\Delta\lambda = 0.1$ was used. A simulation of two periods of $T = 20\,\mu s$ was performed with the initial conditions $V_{C_0} = \begin{bmatrix} -119.96\,V & 139.99\,V & 259.95\,V \end{bmatrix}$, and $I_{L_0} = \begin{bmatrix} 11.77\,A & 11.77\,A & 11.75\,A & 11.75\,A \end{bmatrix}$. We set the resistance of conduction and blocking of the diodes and the transistor in $R_C = 1\,\mu\Omega$ and $R_B = 1\,M\Omega$.

Figure 14(a)(c)(e)(g)(i) and Figure 15(b)(d)(f)(h) illustrate the voltages of the nine nodes. The red points mark the commutations, which are detailed chronologically in Table 3. The black circle encloses the switching point for which the homotopic process has been illustrated to calculate the next topology. Figure 14(b)(d)(f)(h) and Figure 15(a)(c)(e)(g)(i) illustrate the homotopic process performed at the instant $t = 20\,\mu s$. The magenta dots mark the commutations occurring in the homotopic process by varying λ.

Figure 14: (a)(c)(e)(g)(i), time simulation of the boost converter of high gain of voltage level, where red and magenta circles are switching points. (b)(d)(f)(h), homotopic continuation for detect next circuit topology in $t = 20\,\mu s$.

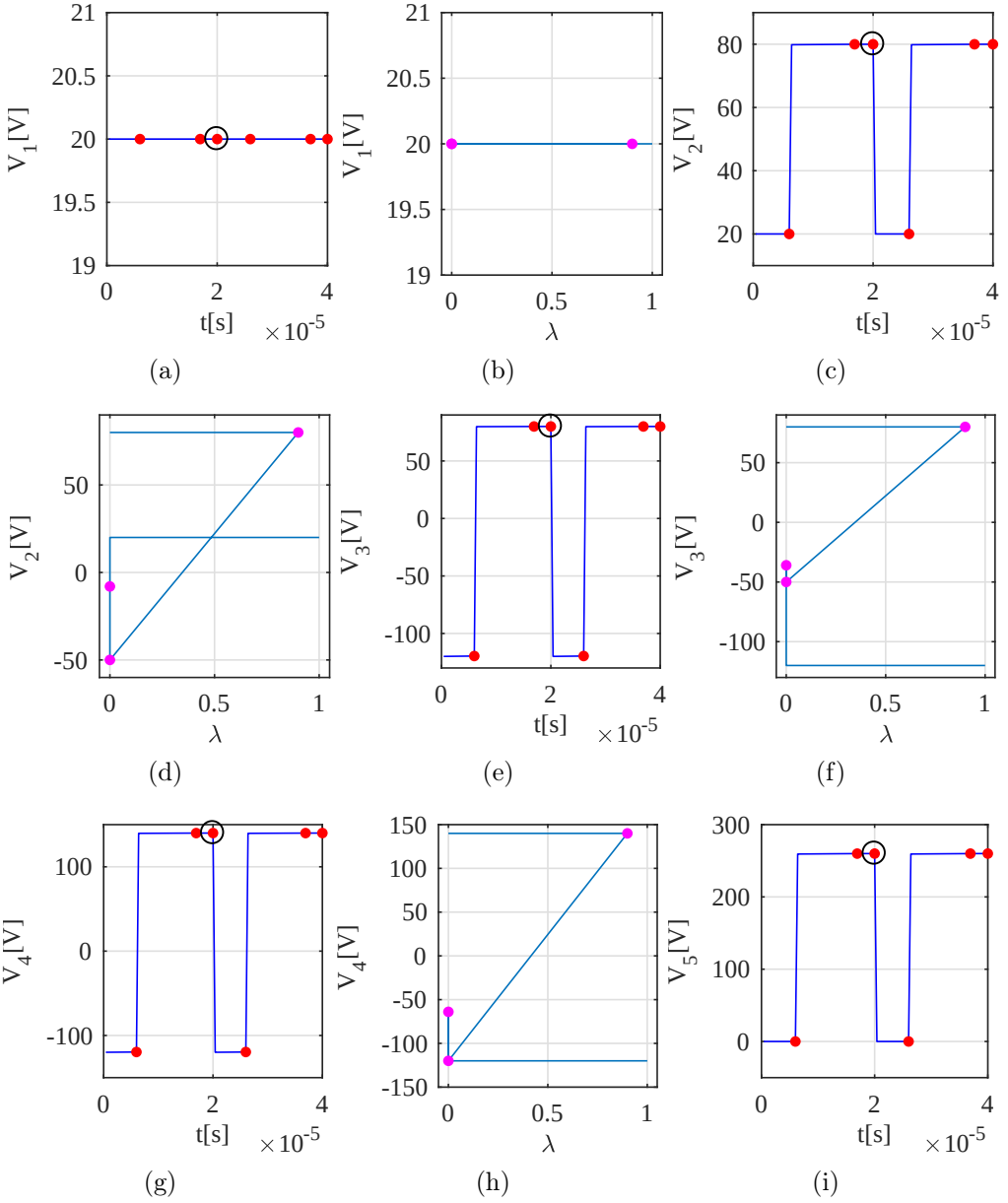

Figure 15: (b)(d)(f)(h), time simulation of the boost converter of high gain of voltage level, where red and magenta circles are switching points. (a)(c)(e)(g)(i), homotopic continuation for detect next circuit topology in $t = 20\,\mu s$.

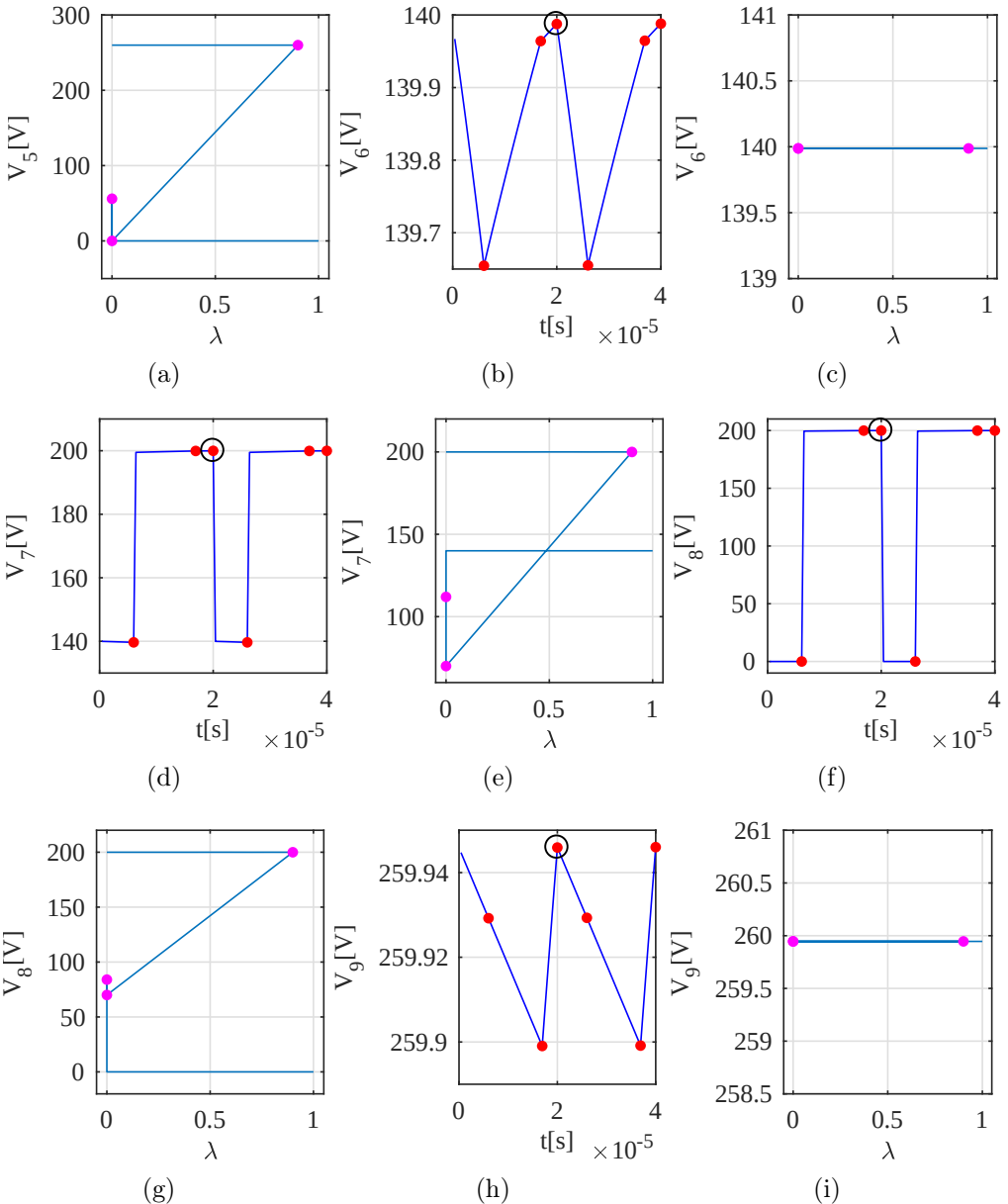

Table 3: Time transitions of the boost converter of high gain of voltage level.

		Next topology								
Time [μs]	Switching device	D_8	D_7	D_6	D_5	D_4	D_3	D_2	D_1	S
6.00	S	0	0	1	0	1	0	1	0	0
16.92	D_8	1	0	1	0	1	0	1	0	0
20.00	S	0	1	0	1	0	1	0	1	1
26.00	S	0	0	1	0	1	0	1	0	0
36.92	D_8	1	0	1	0	1	0	1	0	0

Table 4: Homotopic transitions of the boost converter of high gain of voltage level.

		Next topology								
λ	Switching device	D_8	D_7	D_6	D_5	D_4	D_3	D_2	D_1	S
0.90	D_4, D_8	0	0	1	0	0	0	1	0	1
0.00	D_1, D_3, D_5, D_7	0	1	1	1	0	1	1	1	1
0.00	D_2, D_6	0	1	0	1	0	1	0	1	1

The homotopy starts at the value taken by each voltage before the switching and ends at the value taken after the switching. This is more clearly in those voltages that change abruptly; for instance V_2, Figure 14(c)(d), the voltage just before the commutation analyzed ($t = 20^{-}$ μs) is $V_2\,(t = 20^{-}\,\mu s) = 80\,V$, value in which it also initiates the homotopic process. By varying λ three commutations are presented, first for $\lambda = 0.9$ and then two commutations for $\lambda = 0$ (Table 4). At the end of the homotopy at $\lambda = 1$, the final value of $V_2\,(t = 20^{+}\,\mu s) = 20\,V$ is obtained. This value is observed both in the homotopic and in the time simulation. Both the Newton homotopy and fixed-point homotopy were performed, obtaining exactly the same results for the switching point shown in $t = 20\,\mu s$; for that reason only a homotopy image is presented for each node voltage. All simulations were also performed in PLECS obtaining practically the same results.

Table 5: Computational time (seconds) of each homotopic algorithm, and for each converter.

Algorithm	Boost	Boost–flyback	High gain boost
Newton with hyperspheres	10.32	5.71	–
Hybrid Newton	2.77	1.05	1.61
Hybrid fixed point	2.75	1.01	1.58
Traditional	2.38	0.95	1.55

5 Simulation time comparative

We validated that the voltage signals obtained by homotopic simulations are similar to the signals obtained by the commercial simulator PLECS. Since the homotopic simulations have been implemented in MATLAB code, the computation time is always greater for the algorithms made in MATLAB. However, with the aim of making a comparison in terms of execution times, we implemented the algorithm for the handling of switches presented by Gallo [15]. The main objective of this article is not to make comparisons of execution times, but to offer an alternative to the handling of the commutations.

Table 5 presents the time spent in the simulation of each converter with each one of the homotopic techniques and the traditional one reported in the literature. All algorithms, including the traditional one, were elaborated in MATLAB to make comparisons fairer. The algorithm of Newton with hyperspheres has the longest simulation times for all the converters. The traditional algorithm has the best time, followed closely by the hybrid algorithms.

6 Conclusion

Three homotopic continuation methods were presented for determining the state of switches (diodes and transistor) in power electronic converters after some switching occurrence. These methods describe an intuitive explanation

of how a converter transits through different topologies. Thus, the main advantage offered by homotopic continuation methods is that they trace a clear and deterministic path for the handling of commutations.

The first method used a diode model based on the canonical piecewise linear representation of Chua–Kang. In this proposal, the homotopic tracking was done by means of hyperspheres. The technique was successfully tested on the Boost and Boost–Flyback converters. However, it did not work properly on the high gain Boost converter. The failure is presumed to be due to the high number of diodes (eight). The conventional Boost converter has a single diode, the Boost–Flyback has two and the high gain Boost has eight; which implies a greater number of non-smooth functions that enter the model and that must be solved by the algorithm of Newton–Raphson. The other two implemented homotopic methods employed hybrid models and a uniform parametric sweep, which generated a set of linear topologies that were easy to solve in contrast to the nonlinear models of the first homotopic method. The last two methods could successfully simulate all the proposed converters; however, only the results of the high gain boost converter were shown, which is much more complex and interesting to analyse. In order to validate our proposals, numerical simulations via MATLAB were compared with the results obtained from PLECS, and a good correlation was found with our simulation alternatives.

The first method has proven to be a good choice in the DC analysis of nonlinear electronic circuits. However, for the specific case of electronic converters, it does not seem to be the best alternative. This is because, until now, the simulation results showed that the homotopic tracing by means of hyperspheres had convergence problems for converters of more than three switches. In addition, it was the slowest method of the three studied. On the other hand, the last two methods were able to adequately simulate all the converters. They also presented better times with respect to the first method. The last two methods require hybrid models of the diode. Current commercial simulators specialising in power electronics also use hybrid models. The hybrid models of the diodes generate a set of circuit topologies, which

increases the complexity of the problem. However, each topology is easier to solve individually because it is usually linear in nature, even though the global system is nonlinear.

Regarding the radius of the hyperspheres in the first method, there is still no clear criterion for their estimation. We established its size by numerical experimentation. Therefore, establishing the radius of the hyperspheres systematically is an open problem. The same occurs for the step size determination of the homotopic parameter in the last two methods.

The obtained results support the hypothesis that a power electronic converter is understood as a finite set of continuous subsystems or circuit topologies, where each topology is regarded as a continuous deformation of any other topology.

Acknowledgements This work was supported by Universidad Nacional de Colombia, Manizales, Project 31492 - Vicerrectoría de Investigación, DIMA, and COLCIENCIAS under Contract FP44842-052-2016, and program Doctorados Nacionales 6172-2013.

References

[1] J. H. Alimeling and W. P. Hammer. "PLECS-piece-wise linear electrical circuit simulation for Simulink". In: *Power Electronics and Drive Systems, 1999. PEDS '99. Proceedings of the IEEE 1999 International Conference on*. Vol. 1. 1999, 355–360 vol.1. DOI: 10.1109/PEDS.1999.794588 (cit. on p. E32).

[2] A. El Aroudi and R. Leyva. “Quasi-periodic route to chaos in a PWM voltage-controlled DC-DC boost converter”. In: *IEEE Transactions on Circuits and Systems I: Fundamental Theory and Applications* 48.8 (2001), pp. 967–978. ISSN: 1057-7122. DOI: 10.1109/81.940187 (cit. on pp. E30, E37, E39).

[3] A. El Aroudi and G. Olivar. “Quasi-Periodic Phenomena and Phase-Loqued Orbits in DC-DC Boost Switching Regulators”. In: *15th Triennial World Congress, Barcelona, Spain*. 2002 (cit. on p. E37).

[4] M. Aubry. *Homotopy Theory and Models*. BirkhÃd’user, 1995 (cit. on p. E28).

[5] D. Bedrosian and J. Vlach. “Time-domain analysis of networks with internally controlled switches”. In: *1991., IEEE International Sympoisum on Circuits and Systems*. 1991, 846–849 vol.2. DOI: 10.1109/ISCAS.1991.176495 (cit. on p. E27).

[6] L. Chua and An-Chang Deng. “Canonical piecewise-linear modeling”. In: *IEEE Transactions on Circuits and Systems* 33.5 (1986), pp. 511–525. ISSN: 0098-4094. DOI: 10.1109/TCS.1986.1085952 (cit. on p. E35).

[7] L.O. Chua, C.A. Desoer, and E.S. Kuh. *Linear and Nonlinear Circuits*. Electrical & electronic engineering. McGraw-Hill, 1987. ISBN: 9780071001670. URL: https://books.google.com.co/books?id=hl0pAAAACAAJ (cit. on p. E35).

[8] H. S. H. Chung and A. Ioinovici. “Fast computer-aided simulation of switching power regulators based on progressive analysis of the switches’ state”. In: *IEEE Transactions on Power Electronics* 9.2 (1994), pp. 206–212. ISSN: 0885-8993. DOI: 10.1109/63.286813 (cit. on p. E27).

[9] G. P. Collins. “The Shapes of Space”. In: *Scientific American* (2004), pp. 94–103 (cit. on p. E28).

[10] J. H. B. Deane and D. C. Hamill. "Analysis, simulation and experimental study of chaos in the buck converter". In: *21st Annual IEEE Conference on Power Electronics Specialists*. 1990, pp. 491–498. DOI: 10.1109/PESC.1990.131228 (cit. on p. E27).

[11] N. Femia. "Understanding commutations in switching converters. I. Basic theory and application of the Compensation Theorem". In: *IEEE Transactions on Aerospace and Electronic Systems* 39.1 (2003), pp. 282–297. ISSN: 0018-9251. DOI: 10.1109/TAES.2003.1188911 (cit. on pp. E26, E27, E28, E30).

[12] N. Femia and M. Vitelli. "Time-domain analysis of switching converters based on a discrete-time transition model of the spectral coefficients of state variables". In: *IEEE Transactions on Circuits and Systems I: Fundamental Theory and Applications* 50.11 (2003), pp. 1447–1460. ISSN: 1057-7122. DOI: 10.1109/TCSI.2003.818616 (cit. on pp. E27, E28, E30).

[13] N. Femia and M. Vitelli. "Understanding commutations in switching converters. II. Analysis and synthesis of DC-DC regulators". In: *IEEE Transactions on Aerospace and Electronic Systems* 39.1 (2003), pp. 298–317. ISSN: 0018-9251. DOI: 10.1109/TAES.2003.1188912 (cit. on pp. E26, E27, E28).

[14] F. Florez, J. MuÃśoz, and F. Angulo. "Modeling, simulation and experimental set-up of a boost-flyback converter". In: *2015 IEEE 2nd Colombian Conference on Automatic Control (CCAC)*. 2015, pp. 1–4. DOI: 10.1109/CCAC.2015.7345199 (cit. on pp. E30, E41).

[15] G. Gallo et al. "Automatic hybrid simulation of DC-DC power electronic converters". In: *2017 IEEE 3rd Colombian Conference on Automatic Control (CCAC)*. 2017, pp. 1–6. DOI: 10.1109/CCAC.2017.8276407 (cit. on pp. E30, E46, E51).

[16] M. GÃijnter, U. Feldmann, and E. ter Maten. "Modelling and discretization of circuit problems". In: *Handbook of Numerical Analisys,*

Special Volume on Numerical Methods in Electromagnetics XIII (2005) (cit. on p. E30).

[17] Michiel Hazewinkel. *Encyclopaedia of Mathematics*. Springer, 2001 (cit. on p. E28).

[18] Hugo Jiménez Islas. *Paquete computacional para la solución de ecuaciones no lineales*. 1988 (cit. on p. E28).

[19] S. G. Krantz. *Handbook of Complex Variables*. BirkhÃď user, 1999 (cit. on p. E28).

[20] Héctor Vázquez Leal. "Homotopía doblemente acotada aplicada al análisis en CD de circuitos no lineales". PhD thesis. INAOE, 2005 (cit. on p. E28).

[21] Vesa Linja-aho. *Homotopy Methods in DC Circuit Analysis*. 2006 (cit. on p. E28).

[22] R. D. Middlebrook. "Null double injection and the extra element theorem". In: *IEEE Transactions on Education* 32.3 (1989), pp. 167–180. ISSN: 0018-9359. DOI: 10.1109/13.34149 (cit. on p. E28).

[23] JG Muñoz et al. "Performance Analysis of a Peak-Current Mode Control with Compensation Ramp for a Boost-Flyback Power Converter". In: *Journal of Control Science* (2016). URL: http://www.hindawi.com/journals/jcse/2016/7354791/abs/ (cit. on p. E41).

[24] A. Ramirez-Pinero et al. "Speed-up hyperspheres homotopic path tracking algorithm for PWL circuits simulations". In: *SpringerPlus* 5.1 (2016), p. 890. ISSN: 2193-1801. DOI: 10.1186/s40064-016-2534-5. (Cit. on pp. E28, E33, E37, E39).

[25] O. Bonnefon V. Acary and B. Brogliato. *Nonsmooth Modelind and Simulation for Switched Circuits*. Springer, 2011 (cit. on pp. E27, E30).

[26] F. Vasca and L. Iannelli. *Dynamics and control of switched electronic systems*. Springer, 2012 (cit. on pp. E26, E27, E28, E30).

[27] H. Vazquez-Leal et al. “Modified Hyperspheres Algorithm to Trace Homotopy Curves of Nonlinear Circuits Composed by Piecewise Linear Modelled Devices”. In: *The Scientific World Journal* 2014 (2014). DOI: 10.1155/2014/938598 (cit. on pp. E28, E33, E34).

[28] K. Yamamura. “Simple algorithms for tracing solution curves”. In: *[Proceedings] 1992 IEEE International Symposium on Circuits and Systems*. Vol. 6. 1992, 2801–2804 vol.6. DOI: 10.1109/ISCAS.1992.230616 (cit. on pp. E28, E33).

[29] K. Yamamura, T. Sekiguchi, and Y. Inoue. “A fixed-point homotopy method for solving modified nodal equations”. In: *IEEE Transactions on Circuits and Systems I: Fundamental Theory and Applications* 46.6 (1999), pp. 654–665. ISSN: 1057-7122. DOI: 10.1109/81.768822 (cit. on p. E28).

[30] G. Zhang et al. “An Impedance Network Boost Converter With a High-Voltage Gain”. In: *IEEE Transactions on Power Electronics* 32.9 (2017), pp. 6661–6665. ISSN: 0885-8993. DOI: 10.1109/TPEL.2017.2673545 (cit. on pp. E30, E47).

[31] Song-Ping Zhu. “An exact and explicit solution for the valuation of American put options”. In: *Quantitative Finance* 6.3 (2006), pp. 229–242. DOI: 10.1080/14697680600699811 (cit. on p. E28).

Author addresses

1. **Guillermo Gallo**, Universidad Nacional de Colombia, Sede Manizales, Colombia.
mailto:ggalloh@unal.edu.co
orcid:0000-0002-1253-4961

2. **Hector Vazquez-Leal**, Universidad Veracruzana, Campus Xalapa, México.
mailto:hvazquez@uv.mx

orcid:0000-0002-7785-5272

3. **Victor M. Jimenez-Fernandez**, Universidad Veracruzana, Campus Xalapa, México. *Corresponding author.*
mailto:vicjimenez@uv.mx
orcid:0000-0003-1811-1238

4. **Gustavo Osorio**, Universidad Nacional de Colombia, Sede Manizales, Colombia.
mailto:gaosoriol@unal.edu.co
orcid:0000-0002-8202-6217

5. **Fabiola Angulo**, Universidad Nacional de Colombia, Sede Manizales, Colombia.
mailto:fangulog@unal.edu.co
orcid:0000-0002-4669-7777

6. **Jose A. Martinez-Melchor**, Universidad Veracruzana, Campus Xalapa, México.
mailto:josealfredo@hotmail.es
orcid:0000-0003-4121-0015